Proceedings of the XVII ECSMGE-2019
Geotechnical Engineering foundation of the future
ISBN 978-9935-9436-1-3

doi: 10.32075/17ECSMGE-2019-0466

XVII European Conference
ECSMGE 2019
Reykjavik
on Soil Mechanics
and Geotechnical Engineering

Tunnel face stability laboratory tests in sand considering surface settlements

Étude de laboratoire de la stabilite du front de taille d'un tunnel en sable en considerant les déformations superficielles.

S. Senent
Universidad Politécnica de Madrid, Spain

R. García-Luna, M. Sánchez-Lázaro, R. Jimenez
Universidad Politécnica de Madrid, Spain

ABSTRACT: The results of two tunnel face stability laboratory tests, considering partial collapse and employing a small-scale model at single gravity, are presented. The tunnel is modeled by a rigid cylinder and the collapse of the face is triggered by the retraction of a piston that supports the soil. Both the collapse of the tunnel face and the deformation of the surface are studied. Dry sand with two different relative densities (loose and dense) is employed. By means of the low-cost Structure from Motion photogrammetric technique, a precise three-dimensional model of the material surface is obtained; consequently, it is possible to reproduce the surface settlements during test execution. Results presented herein are primarily focused on the shape of the settlement troughs for loose and dense sand, and on the capability of the Structure from Motion technique for this type of analysis. Additionally, the relationship between the collapse of the tunnel face and the surface settlement is studied. Results show that surface deformations before the activation of the collapse mechanism are small, and mainly depend on the relative density of the material.

RÉSUMÉ: Cet article porte sur les résultats de deux essais de laboratoire sur la rupture partielle du front de taille d'un tunnel, avec un modèle à échelle réduite. Le tunnel est modélisé par un cylindre rigide, afin que la rupture du front soit provoquée par la rétraction d'un piston qui soutient le sol. On etude à la fois l'effondrement du front et les déformations sur la surface du terrain, en utilisant comme matériel d'éssai un sable avec deux densités relatives différentes (soit-disant compacte et lâche). En utilisant la technique photogrammétrique à faible coût "Structure from Motion", on obtient un modèle tridimensionnel précis de la surface du matériau; il est pourtant possible de reproduire les tassements produits pendant l'essai. Les résultats présentés ici portent principalement sur la forme des cuvettes de tassements et sur la capacité de la technique "Structure from Motion" d'enregistrer ce type de test. En plus, on étude la relation entre l'effondrement du front de taille et les tassements. Les résultats montrent que les déformations superficielles avant l'activation du mécanisme de rupture sont faibles et qu'elles dépendent principalement de la densité relative du matériel d'essai.

Keywords: Partial Collapse, Critical Pressure, Structure from Motion.

1 INTRODUCTION

The collapse of a tunnel face may cause dramatic consequences both inside the tunnel, causing risk to workers, and on the surface, particularly in tunnels constructed in urban areas.

Many authors have studied the stability of the tunnel face using laboratory tests, for instance focusing on the collapse geometry and on the calculation of the critical or collapse pressure (e.g., Kirsch, 2010). Although there are many works analyzing surface settlements induced by tunnelling (e.g., Fang et al., 2017), they usually study a 2D tunnel cross section or situations far from collapse. Several works in the literature have also considered the occurrence of a partial collapse, that can occur when two or more materials, with different strength properties, emerge at the tunnel face. However, most previous works have analyzed this topic numerically or analytically (e.g., Vermeer, 2002, Senent and Jimenez, 2015), with only a few experimental works (e.g., Berthoz et al., 2012).

Additionally, many methodologies have been employed to register displacements during tunnel face stability laboratory tests. Some examples are the use of coloured materials or photogrammetric techniques (like Particle Image Velocimetry), the use of transparent materials or, in the case of larger models, the use of classical monitoring techniques. The Structure from Motion (SfM) photogrammetric technique, which is based on the same principles than classical photogrammetry but using redundant photographs that remove the need to calibrate and to orientate the camera, has also been employed in geotechnical laboratory tests. For example, Le et al. (2016) apply it to measure three-dimensional displacements in physical models, using a tunnel face stability model to illustrate the methodology.

In this work we study surface settlements due to partial collapse of the tunnel face using a small-scale laboratory test at single gravity and the SfM technique.

2 METHODOLOGY

2.1 Physical model

Figure 1 shows the set-up of the physical model employed in the laboratory tests, which is practically identical to the one used by Kirsch (2010), with the only difference of dimensions. It consists of a steel frame with four aluminium panels that form the borders of the model. The tunnel is modelled using a 12 cm inner diameter cylinder within which a 11.8 cm diameter aluminium piston can move. The tunnel enters 7 cm into the sand, so that the opposite border is 38 cm (>3 times the tunnel diameter) away. The piston displacement is controlled manually using a micrometre and a load cell installed at the edge of the piston is used to measure the pressure applied by the sand. To avoid that the sand enters in the space between the cylinder and the piston, a plastic foil was placed at the tunnel face. A wooden panel has been placed covering the tunnel face partially to impose a partial collapse, so that only a vertical distance H from the tunnel crown is free to collapse. This wooden panel avoids the collapse of the lower part of the tunnel face, and allows us to simulate a tunnel excavated in a self-stable material with a weaker material appearing in the upper part of the face.

We have employed a silica sand used in glass manufacturing. The particle size distribution is uniform (C_u=1,93) with a mass median diameter d_{50} equal to 0,25 mm. It is a very fine-grain sand which allows to minimize the scale effect according to Garnier et al. (2007) (i.e., the ratio between the tunnel diameter and d_{50} is higher that 175). The unit weight is 2,68 g/cm^3 and the minimum and maximum densities are 1.47 and 1.79 g/cm^3 respectively (i.e., the void ratio varies between 0,50 and 0,82). It is a cohesionless material with a peak frictional angle of 35º and a residual friction angle of 29º.

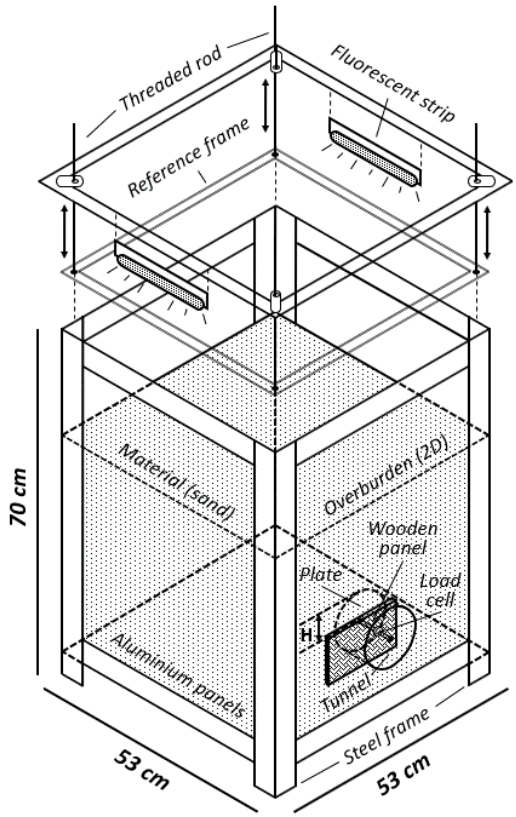

Figure 1. Set-up of the physical model employed in the tunnel face stability laboratory tests.

2.2 Structure from Motion technique

Photogrammetry is a passive remote sensing technique that allows one to accurately capture the shape, dimensions and position of any object, using only photographs of this object. In this work, the "Structure from Motion" (SfM) approach (Snavely et al., 2008) is used. This technique has experienced an enormous development in the recent years, becoming a low-cost alternative to traditional active methods (e.g., LiDAR or Structured light 3D scanning).

The SfM photogrammetric technique allows a direct characterization of reality using photographs resulting from the movement of the sensor/device around the object of study. Unlike conventional stereoscopic photogrammetry, the SfM technique does not need ground control points ---or GCPs, with known x-y-z coordinates--- to solve the photogrammetric restitution process (transformation of 2D data into 3D); it employs only the digital information obtained from the images themselves to model the scene into a 3D point cloud.

2.2.1 Equipment

To apply the SfM technique, only a regular camera and a photogrammetric software that generates the 3D model are needed. In this work, all the images have been taken with a high resolution digital SLR camera (24 MP) model Nikon D5200 with a Nikon NIKKOR AF-S DX lens 18-55 mm F/3.5-5.6G VR (focal length equivalent to 27-82.5 mm in 35 mm film). To simplify data collection, and to improve the stability of the sensor while the photographs were taken, the camera was placed on a Manfrotto professional tripod (height adjustable and high weight) and it was activated by remote control using a wireless device. In addition, to improve lighting conditions during the acquisition of the photographs, and to ensure the correct lighting of the model (avoiding the generation of shadow areas on the sand surface), two fluorescent strips have been installed on two opposite sides of the model, each with a power of 8 W and a luminous flux of 400 lm.

There are several programs for the application of the SfM technique (e.g., Microsoft PhotoModeler or Autodesk ReMake). In this work, the professional version of Agisoft PhotoScan (LCC, 2016) has been used. (Note that the standard version does not allow to work with control points, necessary for comparison between models).

2.2.2 Reference frame

Since we want to analyse the evolution of surface settlements during the tests, all the models generated need to have the same scale and orientation. That is why, although the SfM technique does not generally require the use of

GCPs, in this work they are necessary. Consequently, we introduce a fixed reference surface within the 3D model that is not affected by the tests and that is easily recognizable from the photographs. The GCPs are installed on this reference with the aim of generating a "common" local reference system for all the models, allowing their subsequent comparison. To solve this problem, we have developed a synthetic reference frame, similar to that used by Le et al. (2016), which is located inside the box in direct contact with its walls (Figure 1). This frame has dimensions of 495 x 490 mm and it contains a reference template with 60 GCPs that are printed on a cardboard (Figure 2). (Although theoretically only the relative coordinates of 3 points of the scene are needed to reference the 3D model (LCC, 2016), an increased number improves the density, quality and precision of the final model). The frame of reference must be mobile to be able to adapt to the conditions of each test (i.e., to the overburden modelled). That is why it is attached to the top of the box using 4 threaded steel rods located at the corners, and that allow height adjustments (Figure 1).

3 LABORATORY TESTS

To study the effect of a tunnel face partial collapse on the surface settlements, two laboratory tests have been conducted, one with dense sand and the other with loose sand. In both tests, an overburden (C) of two diameters has been considered, and the contact between the self-stable lower layer and the weaker (unstable) upper layer has been located at the middle height of the tunnel face (H/D = 0.50) (i.e., the wooden panel has been placed covering the lower half of the section). Table 1 lists the material properties and geometrical parameters of each test.

Table 1. Laboratory Tests

Test	Material	C/D	H/D
1	Dense	2	0.5
2	Loose	2	0.5

As indicated, the test is controlled by displacements, so that the collapse of the face is triggered by the retraction of a piston that supports the soil. Each test involves the following steps:

1. Placing the piston in its initial position, covering the tunnel with the plastic foil and placing the wooden panel to impose partial collapse.
2. Filling the box with sand until the required cover (2 diameter) above the tunnel crown is achieved. In the case of dense sand, layers of 4 cm are installed, and they are compacted manually, with 160 uniformly distributed beats applied with a 1,7 kg mallet. In the case of loose sand, it is poured with a small shovel that is kept in contact with the sand. (By means of a small vessel placed at the bottom of the model, the final densities have been measured, obtaining relative densities of 84% and 19% for the dense and loose sand respectively).
3. Installation and levelling (with the aid of two spirit levels) of the reference frame, adjusting its height using the threaded steel rods until it is placed just above the sand surface.
4. Performance of the test, retracting the piston that supports the face. The piston is retracted manually with the help of the micrometer. Displacement increments of 0,025 mm are employed for the first 2,3 mm and with increments of 0.1 mm being used thereafter until a total displacement of 20 mm is achieved

11 photogrammetric models were constructed during the evolution of each test: an initial model before starting the test and 10 intermediate models, corresponding to piston displacement intervals of 2 mm.

4 RESULTS

4.1 Photogrammetric models

28 photographs were taken for each photogrammetric model, performing two complete circular scans around the box using two different focal lengths (Figure 2). Although it is usually assumed that more photographs entail a higher quality model, we wanted to reduce the risk that the movement of personnel around the model to take photographs may affect the test. In addition, García-Luna et al. (2018) show that the quality of a photogrammetric model is more influenced by the quality of the photos than by their number, since lower quality photographs may reduce the accuracy of the final model.

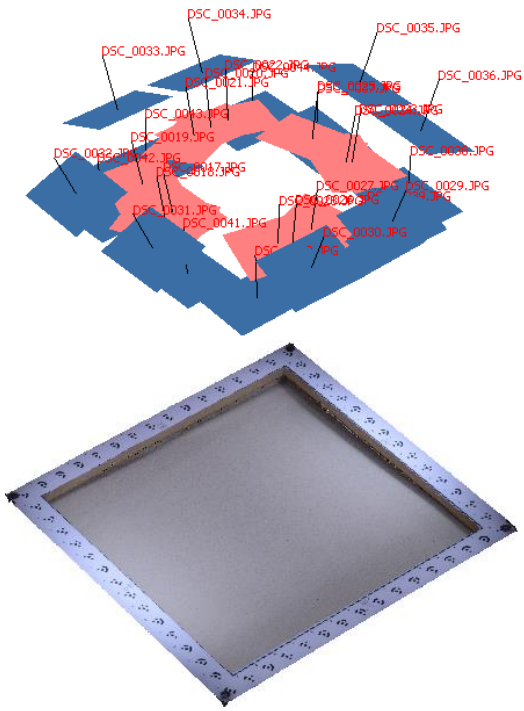

Figure 2. Camera positions for photographs taken in Test 1 (each square indicates a camera position). Red squares: focal length of 26 mm (Scan 1); blue squares: focal length of 55 mm (Scan 2).

To speed up data collection, the photographs were taken using fixed camera adjustments (manual mode, focal length 26-55 mm, center-weighted average metering, MF, image stabilizer off, manual white balance, aperture F/22, exposure time 1/3" and ISO speed rating 100/21°) based on the available lighting conditions of the box. (All photographs were taken with the maximum possible resolution: 24 MP, 3:2; effective pixels 6000 x 4000; JPG format).

The 3D models were generated using the professional version of Agisoft PhotoScan software. All the available images (28) were used in all models. Figure 3 shows two examples of 3D models built using the SfM technique.

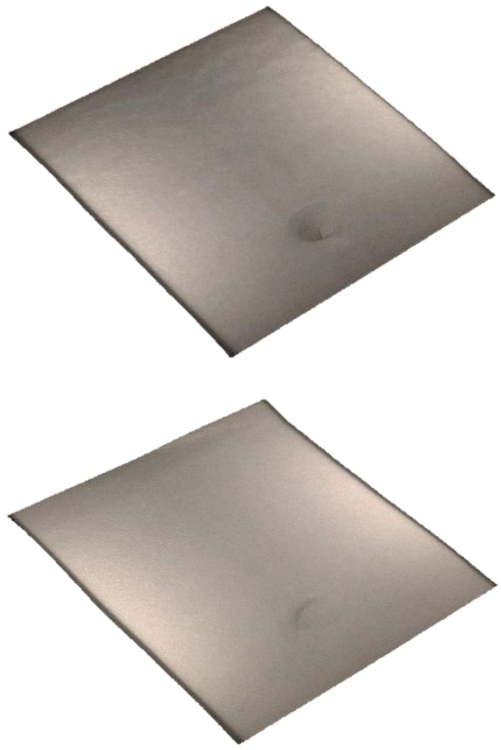

Figure 3. Examples of the photogrammetric 3D models generated with Agisoft PhotoScan (corresponding to the end of each test): (a) dense sand; (b) loose sand.

4.2 Surface settlement analysis

Figure 4 plots, for the two laboratory tests, the final settlement distribution at the model surface

(for a piston displacement of 20 mm). As it can be observed, the settlement trough in dense sand is more concentrated than in loose sand, where the area with settlements higher than 2 mm is more than 5 times larger. In both cases, the settlement distributions are almost circular. Figure 4 also shows that settlements in dense sand exceed 20 mm while in the case of loose sand the maximum settlement is around 14 mm. This fact disagrees with previous results (e.g., Zhou et al., 2014) that shows greater settlements in loose sand. As it is shown below, maximum settlements in dense sand overcome those of loose sand when piston displacement are higher than 13 mm (i.e., for a really significant ground yielding).

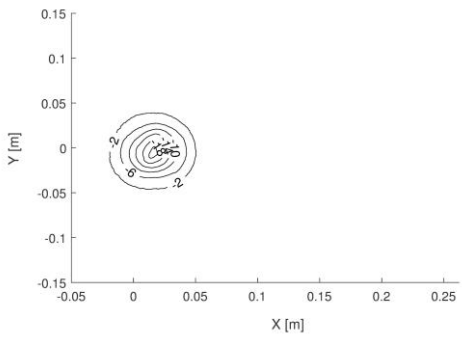

a)

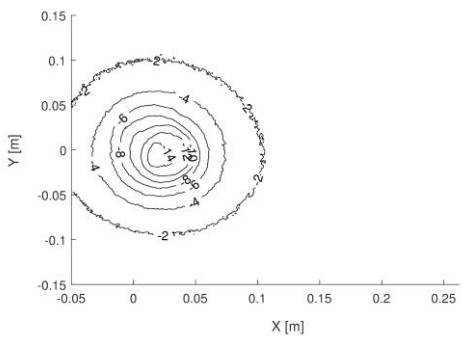

b)

Figure 4. Plan view of surface settlement troughs [mm] at the end of the tests (piston displacement of 20 mm): (a) dense sand; (b) loose sand.

Figure 5 shows the evolution of the settlement troughs during the laboratory tests along a longitudinal section of the model (in the vertical plane of symmetry of the tunnel). As in Figure 4 there are differences between both tests: settlements in dense sand (Figure 5.a) appear in a narrow area and are higher (up to 22 mm), whereas settlements in loose sand (Figure 5.b) extend beyond the edge of the model, but with lower values at the end of the test. Figure 5 also shows the different shapes of the settlement troughs: in dense sand the maximum settlement is clearly differentiated and always in the same location; whereas, in loose sand the settlement produces a Gaussian trough (although other formulations, like modified Gaussian are more suitable; see Marshall et al., 2012) that evolves to a plug geometry, as proposed by Celestino et al. (2009), in the final part of the test.

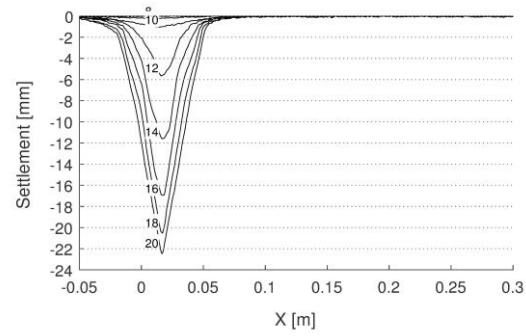

a)

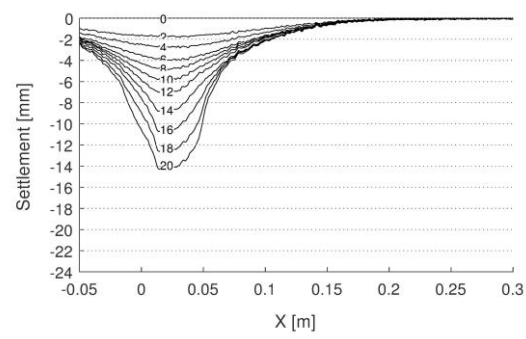

b)

Figure 5. Longitudinal section (along the vertical plane of the symmetry of the tunnel) showing the evolution of surface settlement troughs during the laboratory tests: (a) dense sand; (b) loose sand. (Values next to each curve indicate the related piston displacement, in mm).

Figure 5 also shows that, settlements at the surface of the loose sand model develop significantly since the beginning of the test even for the first photogrammetric model constructed for 2 mm piston displacement. Moreover, settlements continue to increase during the rest of the test. On the other hand, in dense sand, almost no surface settlements occur until the piston has moved 1 cm; thereafter, a sharp settlement trough develops. These results are also plotted in Figure 6, where the evolution of the maximum settlement with the piston displacement is shown. As it can be observed, in loose sand there is an almost linear increment of the maximum settlement as a function of piston displacement, whereas in dense sand the settlement is almost negligible before 8 mm of piston displacement. These results agree with the way the face collapses in frictional materials. As shown by other authors (e.g., Kirsch, 2010), loose sands do no develop a well-defined collapse mechanism, and a diffuse failure zone appears ahead of the tunnel face; dense sands, on the other hand, develop a clearly defined collapse mechanism that ascends as “a chimney” until it outcrops at the surface.

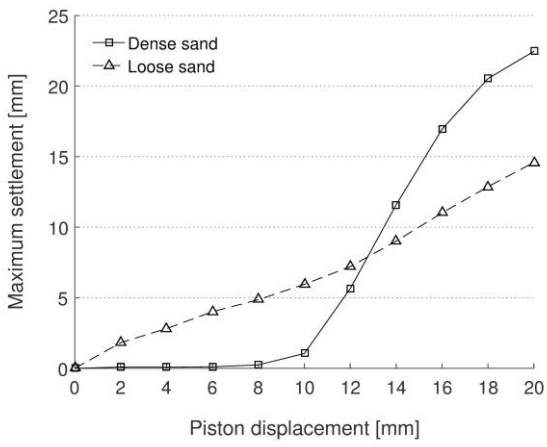

Figure 6. Evolution of maximum settlements as a function of piston displacement, for different sand densities.

Finally, Figure 7 shows the evolution of the pressure registered by the load cell installed in the piston. As it is common in collapse tests (see Terzaghi, 1936), in dense sand the face pressure drops until it reaches a minimum value ---related to the collapse or critical pressure--- from which the pressure increases until a residual value. In loose sand, the face pressure gradually decreases towards a residual value similar to the one given by dense sand. Combining result from Figures 6 and 7, it can be concluded that settlement at the surface before collapse are really small, except perhaps in the case of loose sand.

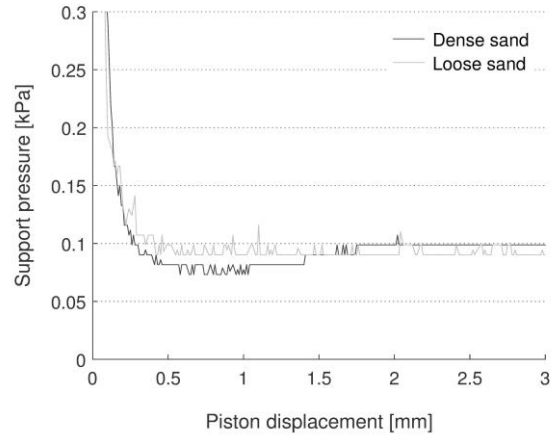

Figure 7. Evolution of registered face pressure as a function of piston displacement, for different sand densities.

5 CONCLUSIONS

We show and discuss results from two laboratory tests about the stability of the tunnel face in sand that were conducted in a small-scale laboratory model, employing two different initial sand densities (dense and loose). A partial face collapse is imposed by a piston that retracts from the tunnel face, while its lower part is supported by a wooden panel that avoids full face collapse. We analyse the evolution of the surface settlements due to the evolution of the collapse, using surface 3D models registered by the low-

cost photogrammetric technique Structure from Motion.

Results show that settlements in dense sand occur in a narrow area, whereas the extension of the settlement trough is larger in loose sand, although final settlement values are lower. Results also show that settlements in loose sand increase continuously as an almost linear function of piston displacement from the beginning of the test, whereas in dense sand the initial settlements are almost negligible and increase sharply in a more brittle way, when the failure mechanism develops after an important piston displacement.

6 ACKNOWLEDGEMENTS

This research was partially supported by the Spanish Ministry of Economy and Competitiveness under Grant BIA2015-69152-R Its support is greatly appreciated.

7 REFERENCES

Berthoz, N., Branque, D., Subrin, D., Wong, H., Humbert, E. (2012). Face failure in homogeneous and stratified soft ground: Theoretical and experimental approaches on 1g EPBS reduced scale model. Tunn. Undergr. Sp. Technol., 30, 25-37.

Celestino, T.B., Gomes, R.A.M.P., Bortolucci, A.A. 2000. Errors in ground distortions due to settlement trough adjustment. Tunn. Undergr. Sp. Technol., 15, 97-100.

Fang, Y., He, C., Nazem, A., Yao, Z., Grasmick, J. 2017. Surface settlement prediction for EPB shield tunneling in sandy ground. Journal of Civil Engineering, 21 (7), 2908-2918.

Kirsch, A. 2010. Experimental investigation of the face stability of shallow tunnels in sand. Acta Geotech., 5, 43-62.

Le, B.T., Nadimi, S., Goodey, R.J., Taylor, R.N. (2016). System to measure three-dimensional movements in physical models. Géotechnique Letters 6, 1-7.

LLC, A., 2016. Agisoft PhotoScan User Manual-Professional Edition. ed. St.Petersburg, Russia. Version 1.2.

Marshall, A.M., Farrell, R., Klar, A., Mair, R. 2012. Tunnels in sand: the effect of size, depth and volume loss on greenfield displacements. Gétoechnique 62 (5), 358-399.

García-Luna, R., Senent, S., Jurado-Piña, R., Jimenez, R. 2018. Structure from Motion photogrammetry to characterize underground rock masses: Experiences from two real tunnels. Tunn. Undergr. Sp. Technol., 83, 262-273.

Senent, S., Jimenez, R. 2015. A tunnel face failure mechanism for layered ground, considering the possibility of partial collapse. Tunn. Undergr. Sp. Technol., 47, 182-192.

Snavely, N., Seitz, S.M., Szeliski, R., 2008. Modeling the world from internet photo collections. Int. J. Comput. Vision 80 (2), 189–210.

Terzaghi, K. (1936). Stress distribution in dry and in saturated sand above a yielding trap-door. Proc., 1st International Conference on Soil Mechanics and Foundation Engineering, Cambridge, Massachusetts, 307-311.

Vermeer, P.A., Ruse, N., Marcher, T. 2002. Tunnel heading stability in drained ground. Felsbau 20, 8-18.

Zhou, B., Marshall, A.M., Yu, H.S. 2014. The effect of relative density on settlements above tunnels in sand. In Geo-Shanghai 2014: Tunnelling and underground construction.